SDRE-Based Integral Sliding Mode Control for Wind Energy Conversion Systems

BAYANDY SARSEMBAYEV[1,2], KANAT SULEIMENOV[1], BOTAGOZ MIRZAGALIKOVA[1], AND TON DUC DO [1], (Senior Member, IEEE)

[1]Department of Robotics and Mechatronics, School of Engineering and Digital Sciences (SEDS), Nazarbayev University, Nur-Sultan Z05H0P9, Kazakhstan
[2]Department of Electronic and Computer Engineering, Brunel University London, Middlesex UB8 3PH, U.K.

Corresponding author: Ton Duc Do (doduc.ton@nu.edu.kz)

ABSTRACT This paper proposes a novel integral sliding mode control (ISMC) scheme based on numerically solving a state-dependent Ricatti equation (SDRE), nonlinear feedback control for wind energy conversion systems (WECSs) with permanent magnet synchronous generators (PMSGs). Unlike the conventional ISMC, the proposed control system is designed with nonlinear near optimal feedback control part to take into account nonlinearities of the WECSs. The Taylor series are used to approximate the solutions of SDRE. More specifically, the nonlinear optimal feedback control has been obtained by solving continuous algebraic Ricatti and Lyapunov equations. Sliding variables are designed such that reaching phase is eliminated and stability is guaranteed. The proposed control method equipped with high-order observer can guarantee more superior results than linear techniques such as linear quadratic regulator (LQR), conventional ISMC, and first-order sliding-mode control (SMC) method. Increasing the number of terms of the Taylor's series of the proposed control law provides better approximation, therefore the performance is improved. However, this increases the computational burden. The effectiveness of the control method is validated via simulations in MATLAB/Simulink under nominal parameters and model uncertainties.

INDEX TERMS Integral sliding mode control (ISMC), state-dependent Ricatti equation (SDRE), permanent magnet synchronous generator (PMSG), wind energy conversion system (WECS), variable-speed wind turbine, generalized high-order disturbance observer (GHODO), nonlinear output feedback, continuous approximation.

I. INTRODUCTION

The disadvantages of the traditional energy sources such as high cost, scarcity, and negative environmental impacts have triggered enormous interest to utilize renewable energy sources effectively. Wind energy is one of the most effective and popular renewable energy sources in the market [1]. Permanent magnet synchronous generator (PMSG) in wind energy conversion systems (WECS) has become popular due to its simple structure, higher reliability, lower maintenance and higher efficiency [2]. In the industrial wind energy conversion systems (WECSs), proportional-integral (PI) controller [3], and linear quadratic regulator (LQR) [4]–[7] have been widely utilized because of their simplicity. However, due to possible parameter/model uncertainties and external disturbances in WECSs, these control

methods cannot guarantee good performance, especially with parameter uncertainties and external disturbance conditions. Although LQR control method is claimed to handle chaotic nonlinear behaviour of electric machine [8], [47], the nonlinear control methods have to be assessed thoroughly. Recently, to cope with limitations of linear control methods, researchers have proposed various advanced linear and nonlinear control techniques to improve performance, attenuate disturbance and unmodelled dynamics in the permanent magnet synchronous generator (PMSG)-based WECS. To overcome these challenges in the nonlinear control systems, the methods such as sliding mode control (SMC) also referred as variable structure control (VSC) [9]–[13], direct torque control (DTC) [14], optimal control [15], fault-tolerant control (FTC) [16], model predictive control (MPC) [17], hybrid control [18], [19], [22], H-infinity control [23], fuzzy control [24], and neural network based control [25], [26], have attracted most attention of research groups in the field.

The associate editor coordinating the review of this manuscript and approving it for publication was Huanqing Wang.

Some of these studies have been devoted to PMSG-based WECSs applications. Among nonlinear control methods, SMC algorithms present a suitable option for its robustness to matched parameters/model uncertainties. However, this method inherited undesirable chattering phenomena [27], [28] because discontinuous function in SMC, which has negative effects on mechanical parts of a system. Although there are many techniques for chattering reduction, the complete elimination is difficult to achieve [29]. For example, the second order SMC control design has been proposed to eliminate chattering in the control system [30]. In addition, traditional SMC consist of two phases, namely, reaching phase and sliding phase. In the reaching phase, a system is vulnerable to parameter uncertainties causing instability of the whole system [31] and may require larger control inputs (gains) to skip this phase [32]. In [13], PI-type sliding surface (SS) with ISMC for 5-phases PMSG has been proposed to control generator-side converter. This control aims to reduce steady state error, and its controllability has been proved by the Lyapunov stability function. The improved PI-type SS for ISMC has been designed to recover nominal transient performance of the control system [12]. In fact, the nominal control law performance can be recovered when model uncertainty presented without asymptotic regulation. Neural network (NN) based nonlinear control method to track the angular shaft speed and torque/currents of PMSG has been proposed in [2]. This design suggests modified Elman NN-based controller, the recurrent weights, connective weights, translations, and dilations trained online via learning algorithm. However, this method should be confined to suggest the mathematical rigor and the feasibility of the nonlinear control methods [33]. DTC based PMSG control technic has been demonstrated for overrated wind speed region via flux weakening technique. While in DTC electromagnetic torque can be controlled directly with space vector modulation (SVM), it has large torque/flux ripples, high acoustic noise at low speed range which lead to poor control performance [34]. Finite-control-set MPC with revised prediction has been proposed to control direct driven PMSG based WECSs with three level neutral-point-clamped back-to-back converter [17]. Although the control variable ripples are reduced, high computational requirement for longer prediction horizon cases is regarded as one of its drawbacks [35]. Moreover, these methods are quite complicated and do not demonstrate detailed steps for implementations, their control techniques can be only verified individually.

While SMC is insensitive to the matched disturbances, the unmatched uncertainties may be present in real physical systems and can destroy stability of sliding mode [36], therefore it requires to use of observers or sensors. The latter causes increasing the price of whole system. Also, for class of nonlinear systems, modified hybrid integral SMC and second order ISMC controllers have been proposed to control inverted pendulum [37], the attitude control of the spacecraft [38], anthromorphic industrial robot manipulator [39], ISMC control law in the studies [10], [40] consists the linear

optimal feedback control as nominal part and continuously approximated discontinuous switching function. However, the nominal control part cannot guarantee better approximation because it does not take into account nonlinear terms of the WECS. In fact, the mathematical model of PMSG based WECS is highly nonlinear system where nonlinear feedback control may provide better performance. Moreover, parameters/model uncertainties in WECS may have additional negative effects to overall performance. Alternatively, to deal with matched and unmatched uncertainties in the nonlinear systems fault-tolerant fuzzy adaptive control scheme with backstepping feature [24], fuzzy ISMC for T–S fuzzy models with dissipativity [20], and nonlinear Markovian jump singular systems [21] have been proposed for class of non-strict-feedback systems with unmodeled dynamics. However, the developed methodologies are very hard to implement in practice because of their high complexity.

Nonlinear optimal control methods are the generalized version of LQR for nonlinear systems. For LQR, it requires to solve algebraic Riccati equation (ARE) to get optimal control gains at each set of weighting matrices. Among nonlinear optimal control approaches, state-dependent Riccati equation (SDRE) based control is quite popular for various nonlinear systems [41]–[47]. In an SDRE based methods, numerical approaches such as Taylor's series expansion can be used to obtain approximated solution of nonlinear optimal controller. Comprehensive studies have shown that SDRE based method is an effective solution to control permanent magnet synchronous motor (SPMSM) [41], [42], doubly fed induction generator (DFIG) [43], free-floating space manipulator [44], mobile robot for obstacle avoidance [45], jet engine compensator, power converter-based DC microgrid, and Vander Pol's oscillator [46].

In this paper, the SDRE-based ISMC control law has been proposed for WECS with PMSG. First, variable speed WECS's model is introduced. Then, SDRE-based nonlinear output feedback control as the nominal part of the proposed control has been proposed. After that, integral–based discontinues function of the proposed control law is continuously approximated and reachability condition is demonstrated. To the best of our knowledge ISMC with SDRE-based nonlinear output feedback has not been applied to control PMSG-side converter in the WECS before. Finally, a design of high-order disturbance observers are presented for estimation of aerodynamic torque as well as disturbances. The SDRE based ISMC method's complexity is not high because of the SDRE terms are solved off-line. All simulations have been implemented in Matlab/Simulink environment.

The remainder of this paper is organized as follows. Section II presents the wind energy conversion system's model. The nonlinear control system design are given in Section III. The generalised high-order disturbance observers follows in Section IV. The effectiveness of the proposed control design is demonstrated and analyzed by simulation results in Section V. Finally, conclusion with further research has been given in Section VI.
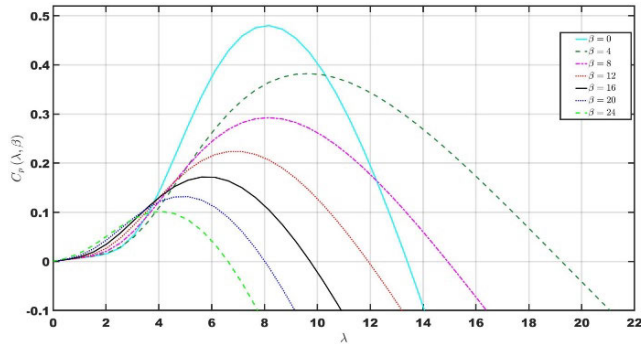
FIGURE 1. Relation of C_p and tip speed ratio λ [18].

II. WIND ENERGY CONVERSION SYSTEM

A. WIND TURBINE MODELLING

A wind turbine (WT) transforms wind kinetic energy into turbine mechanical energy, which, in turn, is converted into electric energy by a generator. Recently, the configuration with a PMSG and full-scale back-to-back (B2B) power converters has been taken over the wind-turbine market to be the dominant solution [17]. The full-scale B2B power converters include two sets of two-level (2L) power converters (PC) named as generator-side and grid-side power converters. In this paper, the *generator-side* PC control system is going to be investigated separately from grid-side one.

The aerodynamic power extracted by WTs is quantified using the following equation [48]

$$P_a = \frac{1}{2}\rho\pi R^2 C_p(\lambda, \beta)v^3 \tag{1}$$

where ρ is the air density, R is the WT rotor radius, v is the wind speed, $C_p(\lambda, \beta)$ is the power coefficient of the wind turbine, which describes the capacity of the turbine to transform the wind kinetic power to mechanical power. The coefficient C_p is a nonlinear function of the tip-speed ratio λ and blade pitch angle β, and it is typically determined experimentally and provided by the manufacturer. The tip-speed ratio is defined as

$$\lambda = \frac{\omega_t R}{v} \tag{2}$$

where ω_t is angular shaft speed of the turbine.

According to (1), WT produces maximum power when C_p is at its maximum, which can be obtained by changing angle β at λ_{opt}. The optimal reference angular shaft speed is defined as follows

$$\omega_{t,d} = \frac{\lambda_{opt}v}{R} \tag{3}$$

Therefore, it is important to track the optimal speed of rotation in order to maximize power harvested from the wind energy.

The gearbox ratio, reflecting the relation between angular speed and torque of the turbine's side and the generator's side is given as follows

$$n_{gb} = \frac{\omega}{\omega_t} = \frac{T_a}{T_{gs}}. \tag{4}$$

The following equation shows the aerodynamic torque obtained from the wind

$$T_a = \frac{P_a}{\omega_t} = \frac{1}{2}\rho\pi R^3 C_q(\lambda, \beta)v^2 \tag{5}$$

where the torque coefficient $C_q(\lambda, \beta) = C_p(\lambda, \beta)/\lambda$.

B. PERMANENT MAGNET SYNCHRONOUS GENERATOR MODEL

It this study, the PMSG was modeled in the *d-q* reference frame. This allows us to simplify the generator model. The dynamic model of PMSG is expressed as follows [3],

$$\begin{cases} J\dfrac{d\omega}{dt} = T_{gs} - B\omega - T_e \\ \dfrac{di_q}{dt} = -\dfrac{R_s}{L}i_q - P\omega i_d - \dfrac{\psi_m P}{L}\omega + \dfrac{1}{L}v_q \\ \dfrac{di_d}{dt} = -\dfrac{R_s}{L}i_d + P\omega i_q + \dfrac{1}{L}v_d \end{cases} \tag{6}$$

where i_d and i_q are the stator currents, and v_d and v_q are the stator voltages in *d*-axis and *q*-axis, respectively; R_s denotes the nominal stator resistance; L is the nominal stator inductance; B stands for the equivalent viscous friction coefficient; ψ_m is the magnet flux linkage; J is the equivalent rotor inertia; P is the number of pole pairs, and T_e is the electromagnetic torque. The electromagnetic torque is then calculated as

$$T_e = Ki_q \tag{7}$$

where $K = 3/2\,\psi_m P$.

The PMSG in the WECS is connected to the wind turbine all the time. This makes the mechanical parameters in the WT very stable and robust to changes. However, the generator's electrical parameters can change with environment temperature or due to friction of the mechanical parts. Considering all uncertainties of stator resistance and inductance, as well as noise, and modeling errors, then combining equations (4), (6), (7), the PMSG dynamic model can take form as follows

$$\begin{cases} \dfrac{d\omega}{dt} = \dfrac{1}{Jn_{gb}}T_a - \dfrac{B}{J}\omega - \dfrac{1}{J}T_e \\ \dfrac{dT_e}{dt} = -PK\omega i_d - \dfrac{R_s}{L}T_e - \dfrac{\psi_m PK}{L}\omega + \dfrac{K}{L}v_q + d_q \\ \dfrac{di_d}{dt} = \dfrac{1}{L}v_d - \dfrac{R_s}{L}i_d + \dfrac{P}{K}\omega T_e + d_d \end{cases} \tag{8}$$

In the system of equations (6) the terms d_q and d_d are included to signify modeling errors, parameter uncertainties, and noise. They are defined as follows

$$d_q = \left(\frac{R_s}{L} - \frac{R_s + \Delta R_s}{L + \Delta L}\right)T_e + \left(\frac{1}{L} - \frac{1}{L + \Delta L}\right)\psi_m PK\omega$$
$$\qquad + \left(\frac{1}{L} - \frac{1}{L + \Delta L}\right)Kv_q + d_{qn} \tag{9}$$

$$d_d = \left(\frac{R_s}{L} - \frac{R_s + \Delta R_s}{L + \Delta L}\right)i_d + \left(\frac{1}{L} - \frac{1}{L + \Delta L}\right)v_d + d_{dn} \tag{10}$$

where ΔR_s and ΔL are the variations of stator resistance and inductance while d_{qn} and d_{dn} are the noise and modeling errors.
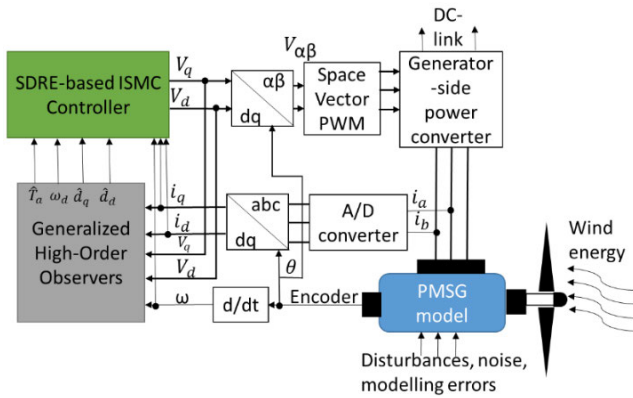
FIGURE 2. Proposed control diagram.

III. NONLINEAR CONTROL SYSTEM DESIGN

A. SDRE-BASED NOMINAL CONTROL PART OF CONTROL

In this section, the nonlinear dynamic model (8) is transformed to the error dynamics form, then the proposed SDRE based ISMC control law will be designed (Fig. 2).

In order to remove reaching phase and make the system less susceptible to the unmodeled dynamics, the ISMC is introduced. By eliminating the reaching phase, the control law becomes imperceptive to the matched disturbances. Let us introduce error dynamics in the following form

$$\tilde{\omega} = \omega - \omega_d, \omega_d = \omega_{t,d} \cdot n_{gb} = \frac{\lambda_{opt}}{R} \vartheta \cdot n_{gb},$$

$$\tilde{T}_e = T_e - T_{ed}, T_{ed} = \frac{1}{n_{gb}} T_a - B\omega_d - J\dot{\omega}_d \quad (11)$$

Let the control inputs V_{qs} and V_{ds} be represented as follows

$$V_{qs} = u_{ffq} + u_{fbq}, V_{ds} = u_{ffd} + u_{fbd} \quad (12)$$

where u_{ffq}, u_{fbq} - q-axis feedforward and feedback control laws, respectively; u_{ffd}, u_{fbd} - d-axis feedforward and feedback control laws, respectively.

The feedforward part of the control laws u_{ffq}, u_{ffd} are defined as

$$u_{ffq} = \frac{R_s}{K} T_{ed} + LP\omega i_d + \psi_m P\omega_d - \frac{L}{K} d_q \quad (13)$$

$$u_{ffd} = -\frac{R_s}{K} \omega T_e - Ld_d \quad (14)$$

Then the initial mathematical model of the WECS in (8) takes the form as follows

$$\begin{cases} \dfrac{d\tilde{\omega}}{dt} = -\dfrac{B}{J}\tilde{\omega} - \dfrac{1}{J}\tilde{T}_e \\ \dfrac{d\tilde{T}_e}{dt} = -PK\tilde{\omega}i_d - \dfrac{R_s}{L}\tilde{T}_e - \dfrac{\psi_m PK}{L}\tilde{\omega} + \dfrac{K}{L}v_q + \hat{d}_q \\ \dfrac{di_d}{dt} = \dfrac{1}{L}v_d - \dfrac{R_s}{L}i_d + \dfrac{P}{K}\tilde{\omega}\tilde{T}_e + \hat{d}_d \end{cases} \quad (15)$$

By using above equations the state-space model can be formed as,

$$\dot{x} = A(x)x + B(u - u_c) \quad (16)$$

where $x = [\tilde{\omega}\,\tilde{T}_e i_d]^T$ the system state vector; $A(x)$ is continuous matrix for all x's and B is constant control matrix;

$u = [u_q u_d]^T$ - control input; u_c – compensating term.

$$A(x) = \begin{bmatrix} -\dfrac{B}{J} & -\dfrac{1}{J} & 0 \\ -\dfrac{\psi_m PK}{L} & -\dfrac{R_s}{L} & -PK\tilde{\omega} \\ 0 & \dfrac{P}{K}\tilde{\omega} & -\dfrac{R_s}{L} \end{bmatrix}, \quad B = \begin{bmatrix} 0 & 0 \\ \dfrac{K}{L_s} & 0 \\ 0 & \dfrac{1}{L_s} \end{bmatrix} \quad (17)$$

The matrix $A(x)$ in the equation (17) can be casted as following

$$A(x) = A_0 + \Delta A(x). \quad (18)$$

To have the state matrix $A(x)$, which can be split into two parts: constant matrix A_o and state-dependent incremental matrix $\Delta A(x)$.

$$A_0 = \begin{bmatrix} -\dfrac{B}{J} & -\dfrac{1}{J} & 0 \\ -\dfrac{\psi_m PK}{L} & -\dfrac{R_s}{L} & 0 \\ 0 & 0 & -\dfrac{R_s}{L} \end{bmatrix},$$

$$\Delta A(x) = \begin{bmatrix} 0 & 0 & 0 \\ 0 & 0 & -PL\tilde{\omega} \\ 0 & \dfrac{PL}{K}\tilde{\omega} & 0 \end{bmatrix}, \quad B = \begin{bmatrix} 0 & 0 \\ \dfrac{K}{L_s} & 0 \\ 0 & \dfrac{1}{L_s} \end{bmatrix}$$

For the system (16) the control input has to be designed such that

$$u(t) = u_{SDRE}(t) + u_1(t) \quad (19)$$

where $u_{SDRE}(t)$ is SDRE-based the nominal control part, and $u_1(t)$ is integral based discontinuous part to eliminate reaching phase and to facilitate robust control of unmeasured matched disturbance.

Allowing the nonlinearities in the system, SDRE creates the nonlinear output feedback control in the system. Its flexibility is defined by the use of state-dependent weighting matrix. The Taylor series expansion can be used to obtain approximated solution of nonlinear dynamics. The coefficients of the Ricatti equations vary in a point-wise manner.

As the state and input weighting matrix of equation (18) are assumed to be state dependent, **care** and **lyap** Matlab solvers are applied to design the nominal part of the proposed control law. It is applied in a point-wise manner and tends to minimize cost function (20) and drive control system to the origin.

$$J = \int_0^\infty \left[x^T Q x + u^T R u \right] dt \quad (20)$$

where Q– state-cost weighted matrix and R -input-cost weighted matrix.

Thus, the near optimal nominal part of control law which minimizes the performance index can take the form:

$$u = -K(x)x = R^{-1}B^T P(x)x, K : \mathcal{R}^n \to \mathcal{R}^{p \times n} \quad (21)$$

where $P : \mathcal{R}^n \to \mathcal{R}^{n \times n}$ satisfies ARE and for the given system the control function (21) $P(x)$ is a unique symmetric and positive definite solution of the following SDRE:

$$P(x)A(x) + A(x)^T P(x) - P(x)BR^{-1}B^T P(x) + Q = 0 \quad (22)$$

As a result, the state-dependent optimal gain matrix K can also be expressed as the sum of constant and state-dependent matrices:

$$u_{SDRE}(t) = -(K_0 + \Delta K(x))x \quad (23)$$

where

$$K_0 = R^{-1}B^T P_0 \quad \Delta K(x) = R^{-1}B^T \Delta P(x) \quad (24)$$

The detailed stability analysis for state-dependent Ricatti equation can be found in [41].

B. SOLVING OF SDRE-BASED ISMC CONTROLLER BY TAYLOR SERIES METHOD

Similar to the works [41], [42] by applying Taylor series method the approximated solution of SDRE-based nominal part of ISMC of the proposed control law can be expressed as

$$u^N(x) = -R^{-1}B^T \left(\sum_{n=0}^{N} (g(x))^n (P_n)_C \right) x$$

$$= -\left(\sum_{n=0}^{N} (g(x))^n K_n \right) x, \quad (25)$$

where $K_n = R^{-1}B^T (P_n)_C$, N is the number of members in series computed offline, and $(P_n)_C$ is a constant matrix, achieved by solving the following algebraic Riccati and Lyapunov equations:

$$P_0^C A + A^T P_0 - P_0 B R^{-1} B^T P_0 + Q = 0 \quad (26)$$

$$(P_1)_C \left(A - B R^{-1}B^T P_0 \right) + \left(A^T - B R^{-1}B^T P_0 \right)(P_1)_C$$
$$+ P_0 \Delta A_C + \Delta A_C P_0 = 0 \quad (27)$$

$$(P_n)_C \left(A - B R^{-1}B^T P_0 \right) + \left(A^T - B R^{-1}B^T P_0 \right)(P_n)_C$$
$$+ (P_{n-1})_C \Delta A_C + \Delta A_C^T (P_{n-1})_C$$
$$- \sum_{k-1}^{n-1} P_k B R^{-1}B^T (P_{n-1})_C = 0 \quad (28)$$

with $A_1 = A_0 - B R^{-1}B^T P_0$, and

$$\Delta A_C = \begin{bmatrix} 0 & 0 & 0 \\ 0 & 0 & -PL \\ 0 & \dfrac{PL}{K} & 0 \end{bmatrix} \quad (29)$$

C. DESIGN OF DISCONTINUOUS CONTROL PART OF SDRE-BASED ISMC CONTROL LAW

In this subsection, discontinuous function of the proposed SDRE-based ISMC will be presented. The task is to design the integral-based discontinues control part which will drive sliding variable to zero in order to guarantee sliding mode in finite time and eliminate reaching phase.

Shall (16) will be formed as

$$\dot{x}(t) = A(x)x + B(u - u_c) + L\epsilon(t, x) + d_u(t, x) \quad (30)$$

where $\epsilon(t)$ and $d_u(t, x)$ are matched and mismatched disturbances, respectively. $L = BD$ for $D \in R$.

By substituting (19) into (30), obtained following

$$\dot{x}(t) = A(x)x + B u_{SDRE}(t) - B u_C(t)$$
$$+ B u_1(t) + BD\epsilon(t, x) + d_u(t, x) \quad (31)$$

The sliding variable includes integral term as:

$$\sigma(x) = Gx(t) + w(t) \quad (32)$$

where G is a design matrix $(G = (B^T B)^{-1} B^T)$, $w(t)$ is an integral term.

During sliding mode, the sliding variable and its derivatives must be zero as

$$\dot{y}(x) = G\dot{x}(t) + \dot{w}(t) = 0 \quad (33)$$

By substituting (31) into (33) the following is obtained

$$\dot{\sigma}(t) = G(A(x)x + B u_{SDRE}(t)) + GBu_1(t)$$
$$+ GBD\epsilon(t, x) + Gd_u(t, x) + \dot{w}(t) = 0 \quad (34)$$

During sliding mode discontinuous part of control law is

$$u_1(t) = -D\epsilon(t, x) - (GB)^{-1} Gd_u(t, x) \quad (35)$$

The derivative of the integral term of sliding variable should be selected as

$$\dot{w}(t) = -G(Ax(t) + B u_{SDRE}(t)) \quad (36)$$

Finally, integral siding variable will be as

$$\sigma(x) = G(x(t) - x(0))$$
$$- G \int_0^t (Ax(t) + B u_{SDRE}(t)) \, dt \quad (37)$$

To reduce chattering presented in ISMC, continuous approximation using Euclidian norm is utilized similar to [29].

$$u_1(t) = -\rho \frac{\sigma(t)}{\|\sigma(t)\| + \delta}. \quad (38)$$

It should be noted that the obtained suboptimal control solution of the optimal control problem related to nonlinear dynamics using (19), (21) and (38) is subject to the linear quadratic performance index given in (20).

To justify, the controller designed in (37) satisfies the η-reachability condition that ensures the existence of an ideal sliding motion [49].

Let take Lyapunov's candidate function as

$$V(t) = \frac{1}{2}\sigma^T(t)\sigma(t) \quad (39)$$

Then

$$\dot{V}(t) = \sigma^T(t)\dot{\sigma}(t) \quad (40)$$

And

$$\dot{\sigma}(t) = G(Ax(t) + Bu(t) + BD\xi(t, x)$$
$$+ f_u(t, x)) - GAx(t) - GBFx(t) \quad (41)$$

After reforming and substituting (37) into (41) is obtained

$$\dot{\sigma}(t) = GAx(t) + GB(-Fx(t) + u_c(t)) + GBD\xi(\cdot)$$
$$+ Gd(\cdot) - GAx(t) + GBFx(t) =$$
$$= -\rho(t, x)\frac{\sigma(t)}{\|\sigma(t)\|} + GBD\xi(t, x) + Gf_u(t, x) \quad (42)$$

where F is SDRE – based nonlinear output feedback control which is responsible for the performance of the system after

TABLE 1. WECS parameters.

Symbol	Quantity	Value	[Unit]
P_{rated}	Rated power	5	kW
R_s	Stator resistance	0.3676	Ω
L	Stator inductance	3.55	mH
ψ_m	Magnet flux linkage	0.2867	V·s/rad
J	Mechanical inertia	7.856	kg·m²
P	Pole pairs	14	-
B	Viscous friction coefficient	0.002	kg·m²/s
R	Rotor radius	1.84	m
ρ	Air density	1.25	kg/m³

TABLE 2. Control system parameters.

Controllers and Observers, solver type	Parameters and Gains
ISMS: nominal part gains	Q=diag([5000 10 1]), R=diag([1 1])
SDRE terms, N	2
Matlab solver type	care & lyap
ISMC: discontinuous part gains	ρ_1=100, ρ_2=100
Small value for continues approximation	δ=0.001
T_a observer gains	Y_{01}=50, Y_{02}=250, Y_{03}=500
d_q –axis disturbance observer's gains	Y_{01}=200, Y_{02}=500, Y_{03}=1000
d_d –axis disturbance observer's gains	Y_{01}=200, Y_{02}=500, Y_{03}=1000

reaching sliding phase and $\rho(t,x)$ is gain of discontinuous function to enforce the sliding mode. Then

$$\sigma^T(t)\dot{\sigma}(t) = -\rho(t,x)||\sigma(t)|| + \sigma^T(t)D\xi(t,x)$$
$$+ \sigma^T(t)Gf_u(t,x)$$
$$\leq ||\sigma(t)||(-\rho(t,x) + ||D\xi(t,x)||$$
$$+ ||Gfu(t,x)||) \qquad (43)$$

where the fact that $GB = I_m$, has been used. In order to enforce a sliding mode the value of the modulation gain $\rho(t,x)$ should be greater than any disturbance or uncertainty in the system, and therefore for any choice of $\rho(t,x)$ which satisfies

$$\rho(t,x) \geq ||D|| \, ||\xi(t,x)|| + ||G|| \, ||f_u(t,x)|| + \eta \quad (44)$$

where η is some positive scalar, the η-reachability condition

$$\sigma^T(t)\dot{\sigma}(t) \leq -\eta||\sigma(t)|| \qquad (45)$$

is satisfied.

IV. GENERALIZED HIGH-ORDER DISTURBANCE OBSERVER DESIGN

In this section, the main concept of GHODO design is presented for the case of fast-varying disturbance. Although the use of traditional anemometers to measure wind speed seems simple solution, the observers to measure aerodynamic torque is not only cost-efficient solution, but also provides high accuracy of measurement. Using unappropriate observers lead to overall poor performance and less accuracy of whole control. Although in many research publications, it is stated that the fast-changing disturbance does not greatly affect to the systems, it has not been observed zero errors at the steady-state. The high-quality observer along with controller can provide good performances of the control system. Therefore, the use of GHODO is considered as one of the appropriate solutions to estimate aerodynamic torque and disturbances on *d-q* axes rather the use of anemometers [4].

Assumption: The external disturbance, aerodynamic torque (T_a) and model uncertainties (d_q, d_d) are fast-changing, but are smooth enough. There are positive integers k_i such that $T_a, d_q, d_d \in C^{k_i+1}(i = 1, 2, 3)$. Moreover, $(k_i + 1)$- order derivatives of T_a and d_q, d_d are ignorable, $\frac{dM^{k_i+1}}{dt^{k_i+1}} \approx 0$ $(i = 1, 2, 3; M = T_a, d_q, d_d)$.

A. AERODYNAMIC TORQUE AND ANGULAR SHAFT SPEED REFERENCE ESTIMATION

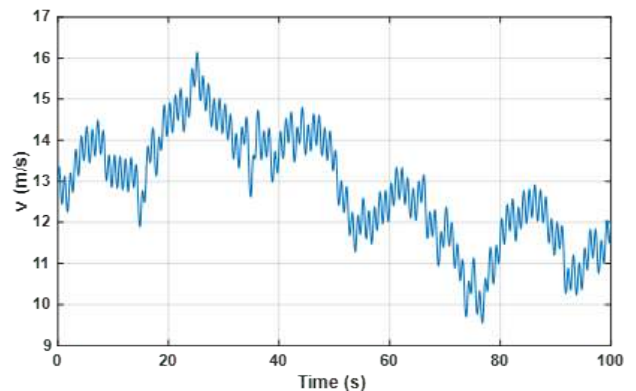To estimate aerodynamic torque for estimation wind speed the PMSG rotor's speed dynamic equation (8) has

FIGURE 3. Wind speed (v) profile with mean speed of 12.13 (m/s).

to be recalled

$$\frac{d\omega}{dt} = \frac{1}{Jn_{gb}}T_a\frac{B}{J}\omega - \frac{1}{J}T_e \qquad (46)$$

Then, the generalized high-order aerodynamic torque observer is designed as in [4]

$$\begin{cases}
\dot{Z}_\omega = -n_{gb}(B\omega + T_e) + \hat{T}_a \\
\hat{T}_a = L_{01}g_{01} + L_{11}g_{11} + \ldots + L_{k_11}g_{k_11} \\
g_{01} = Jn_{gb}\omega - Z_\omega \\
\dot{g}_{11} = g_{01} \\
\dot{g}_{21} = g_{11} \\
\quad \vdots \\
g_{k_11} = g_{(k_1-1)1},
\end{cases} \qquad (47)$$

where $(\hat{\cdot})$ and $(\dot{\cdots})$ denotes the estimation and 1st order derivative of the argument functions, respectively, L_{01}, L_{11}, L_{k_11} are aerodynamic observer gains.

From this using (5) and (11) the estimation of angular shaft speed reference can be defined as following

$$\hat{\omega}_d = \sqrt{\frac{\hat{T}_a}{k_{opt}}}, \qquad (48)$$

where $k_{opt} = \frac{\rho\pi R^5 C_{pmax}}{2\lambda_{opt}^3 n_{gb}^2}$.

B. MODEL UNCERTAINTY ESTIMATION

To estimate disturbances associated with model uncertainties, modeling errors, and noise, the PMSG T_e and i_d dynamic

TABLE 3. Simulation scenarios.

Scenario	Details
1	Nominal parameters in Table 1
2	$R_s = +20\%$, $L = -1\%$

TABLE 4. SDRE-based ISMC control performance.

Parameter error	Method	Scenario 1	Scenario 2
Average absolute angular shaft speed tracking error, $|\tilde\omega|$, %	SDRE +ISMC, N=1	0.232	0.2337
	SDRE +ISMC, N=2	0.0702	0.0621
	LQR [4]	0.3207	0.3204
	ISMC [10]	0.319	0.3182
	SMC[29]	0.2918	0.2916
Average absolute electromagnetic torque tracking error, $|\tilde T_e|$, %	SDRE +ISMC, N=1	3.5697	3.5933
	SDRE +ISMC, N=2	1.1709	1.0398
	LQR [4]	4.9262	4.9237
	ISMC[10]	4.9054	4.8938
	SMC[29]	4.8345	4.8312

equations from (8) have to be recalled

$$\begin{cases} \dfrac{dT_e}{dt} = -PK\omega i_d - \dfrac{R_s}{L}T_e - \dfrac{\psi_m PK}{L}\omega + \dfrac{K}{L}v_q + d_q \\ \dfrac{di_d}{dt} = \dfrac{1}{L}v_d - \dfrac{R_s}{L}i_d + \dfrac{P}{K}\omega T_e + d_d \end{cases} \quad (49)$$

From above the following generalized high-order disturbance observers can be deduced. For estimation of the disturbance in q-axis

$$\begin{cases} \dot Z_{T_e} = -PK\omega i_d - \dfrac{R_s}{L}T_e - \dfrac{\psi_m PK}{L}\omega + \dfrac{K}{L}v_q + \hat d_q \\ \hat d_q = L_{02}g_{02} + L_{12}g_{12} + \ldots + L_{k_22}g_{k_22} \\ \dot g_{02} = T_e - Z_{T_e} \\ \dot g_{12} = g_{02} \\ \dot g_{22} = g_{12} \\ \quad \vdots \\ g_{k_22} = g_{(k_2-1)2} \end{cases} \quad (50)$$

where L_{02}, L_{12}, L_{k_22} are q-axis disturbance observer gains.
For estimation of the disturbance in d-axis

$$\begin{cases} \dot Z_{i_d} = \dfrac{1}{L}v_d - \dfrac{R_s}{L}i_d + \dfrac{P}{K}\omega T_e + \hat d_d \\ \hat d_d = L_{03}g_{03} + L_{13}g_{13} + \ldots + L_{k_33}g_{k_33} \\ \dot g_{03} = i_d - Z_{i_d} \\ \dot g_{13} = g_{03} \\ \dot g_{23} = g_{13} \\ \quad \vdots \\ g_{k_33} = g_{(k_3-1)3} \end{cases} \quad (51)$$

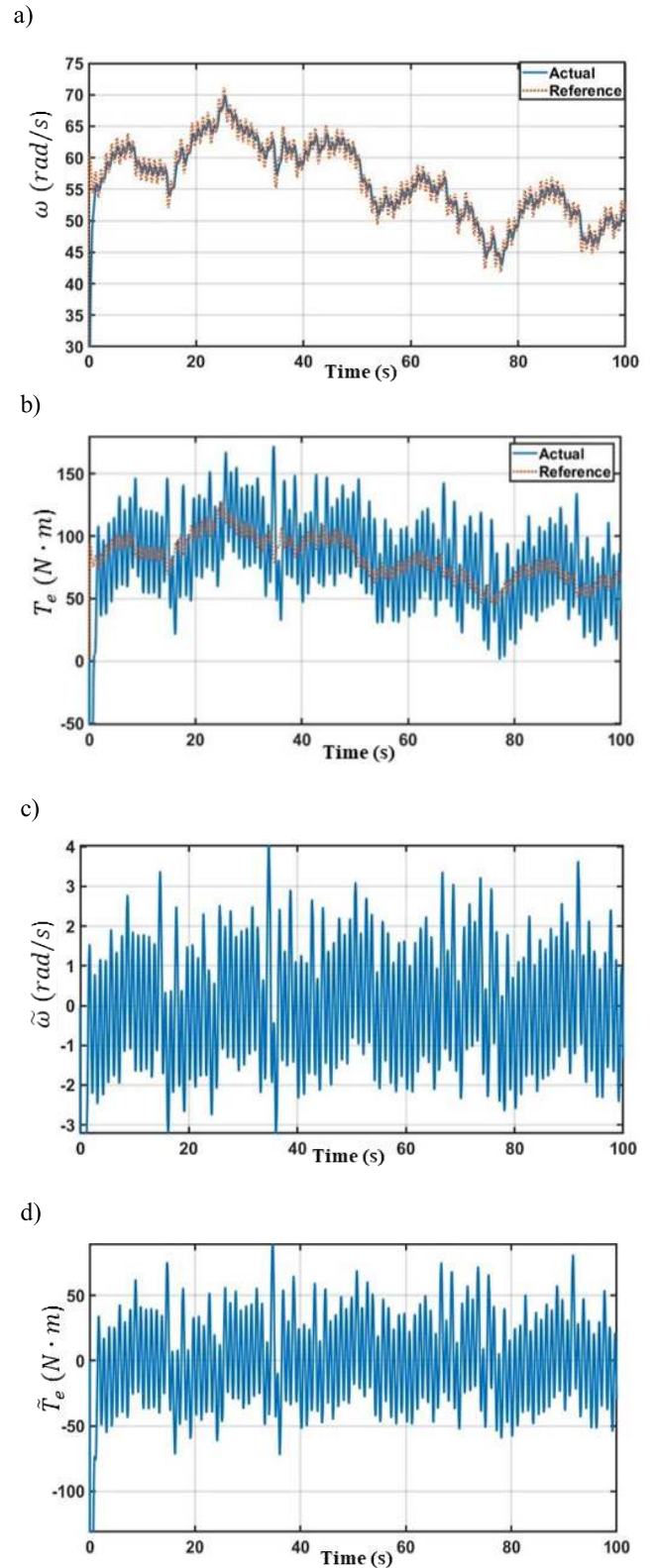where L_{03}, L_{13}, L_{k_33} are d-axis disturbance observer gains.

a)

b)

c)

d)

FIGURE 4. Scenario 1: (a) ω, angular shaft speed tracking, (b) T_e, electromagnetic torque tracking, (c) $\tilde\omega$ angular shaft speed tracking errors, (d) $\tilde T_e$, electromagnetic torque tracking with proposed control, N = 1.

The detailed explanations on how to choose the gains for stability and less steady-state errors with GHODO are given in [4].
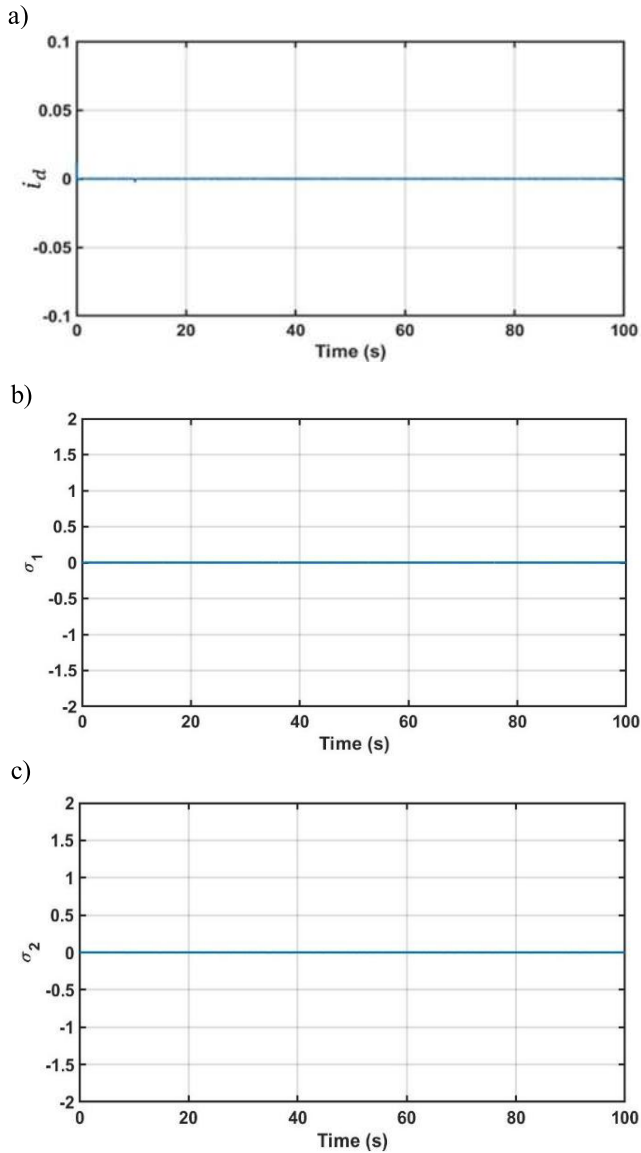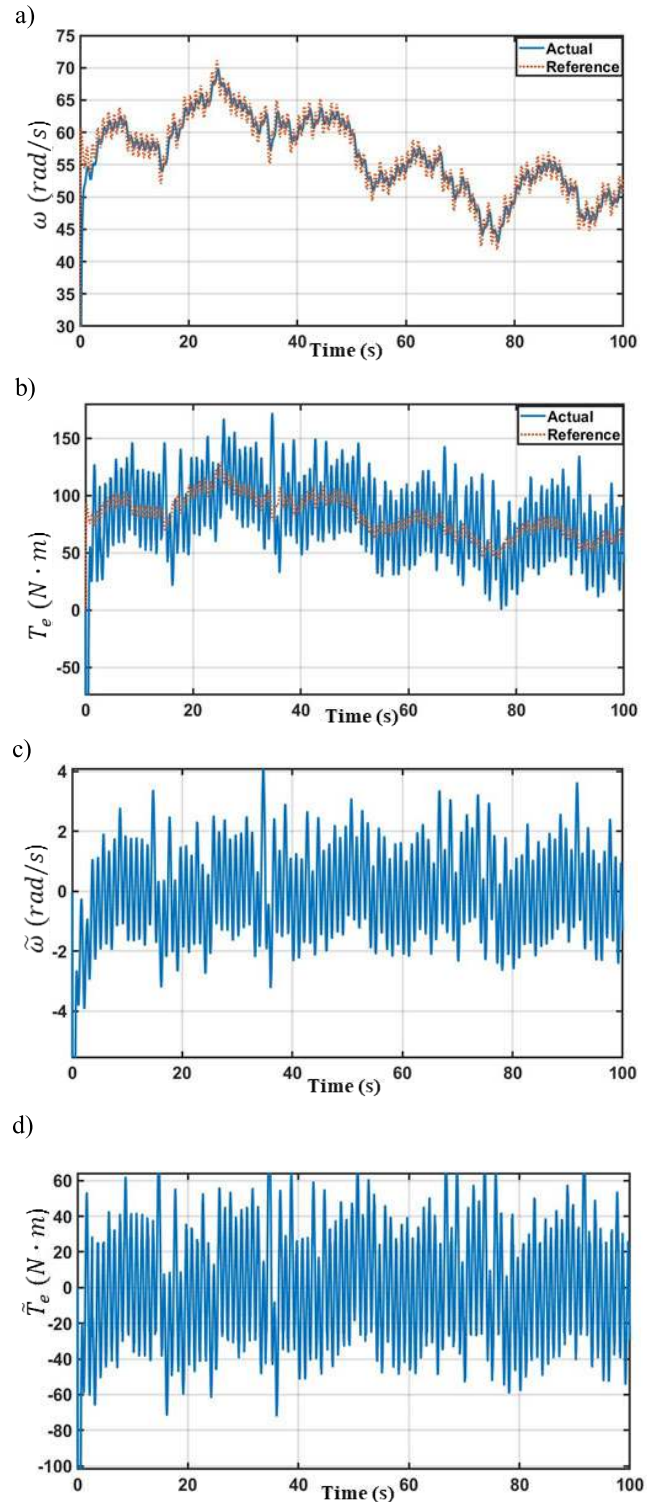
FIGURE 5. Scenario 1: (a) i_d, d-axis current, (b) σ_1 sliding surface and (c) σ_2 sliding surface convergence to zero with proposed control, N =1.

V. RESULTS AND DISCUSSION

In order to apply the proposed control scheme, the Matlab/Simulink simulation model of WECS has been designed. The small power WECS parameters are given in Table 1. Control parameters which have been used in simulations are presented in Table 2. Wind speed profile is shown in Fig. 3. The mean value of 12.13 [m/s] of wind profile is given according to study [41]. The power coefficient C_p is analytically estimated and defined as $\lambda_{opt} = 8.09$ and $C_{pmax} = 0.3262$. To consider the performance of the proposed control method under parameters uncertainties, the stator resistance is increased by 20% and inductance is reduced by 1% (Table 3). Also, to evaluate the control system under noise and modelling errors, $d_{qn} = 10^5 sin(t)$ and $d_{dn} = 10^3 sin(t)$ have been injected to the system.

FIGURE 6. Scenario 1: (a) ω, angular shaft speed tracking (b) T_e, electromagnetic torque tracking (c) $\tilde{\omega}$ angular shaft speed tracking errors and (d) $\tilde{T}_e$, electromagnetic torque tracking with proposed control, N = 2.

By solving ARE equations (26) and Lyapunov equation (28) and (29) with $N = 2$, number of terms in Taylor's series, the near optimal gains matrices are obtained
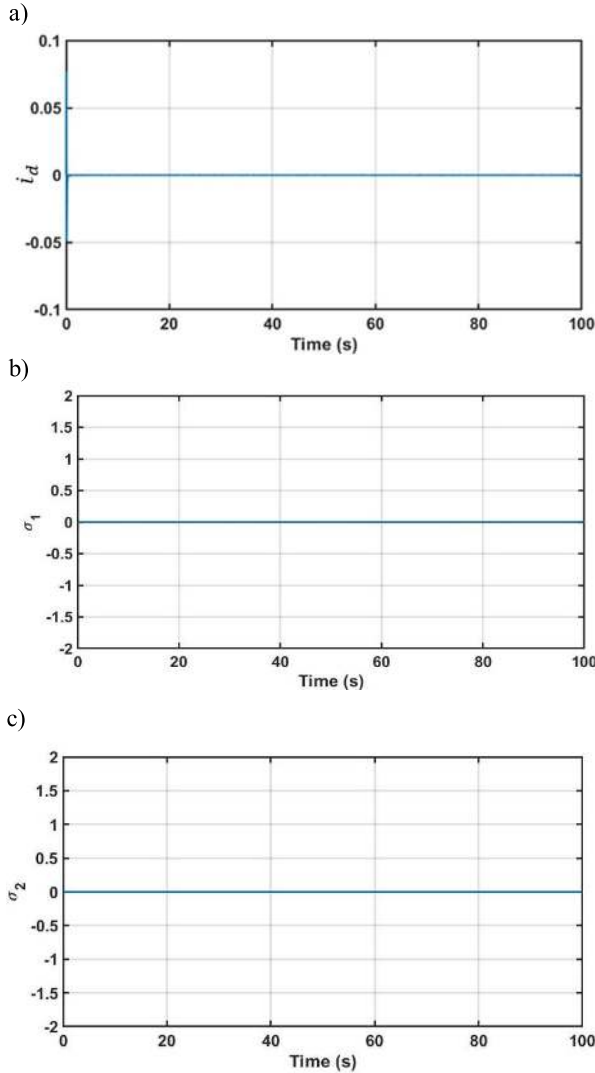
a)

b)

c)

FIGURE 7. Scenario 1: (a) i_d, d-axis current, (b) σ_1 sliding surface and (c) σ_2 sliding surface convergence to zero with proposed control, N = 2.

as follows

$$K_0 = \begin{bmatrix} -74.8320 & 3.1036 & -0.0000 \\ 0.0000 & -0.0000 & 0.6978 \end{bmatrix}$$

$$K_1 = \begin{bmatrix} 0.0000 & 0.0000 & 0.2603 \\ 0.0020 & 0.0432 & -0.0000 \end{bmatrix}$$

$$K_2 = \begin{bmatrix} -0.0277 & -0.6206 & 0.0000 \\ 0.0000 & 0.0000 & -0.0318 \end{bmatrix}$$

The simulations of SDRE-based ISMC for WECS with permanent magnet synchronous generator shows considerable stability results under some parameters variations, better flexibility in choosing the control parameters.

The superior performance of the proposed SDRE-based ISMC controller are presented in Table 4 (Figs. 4-13). The performance has been assessed by percentage of average absolute angular shaft speed tracking error $|\tilde{\omega}|$ and percentage of average absolute electromagnetic torque error $|\tilde{T}_e|$ function of the quadrature current i_q.
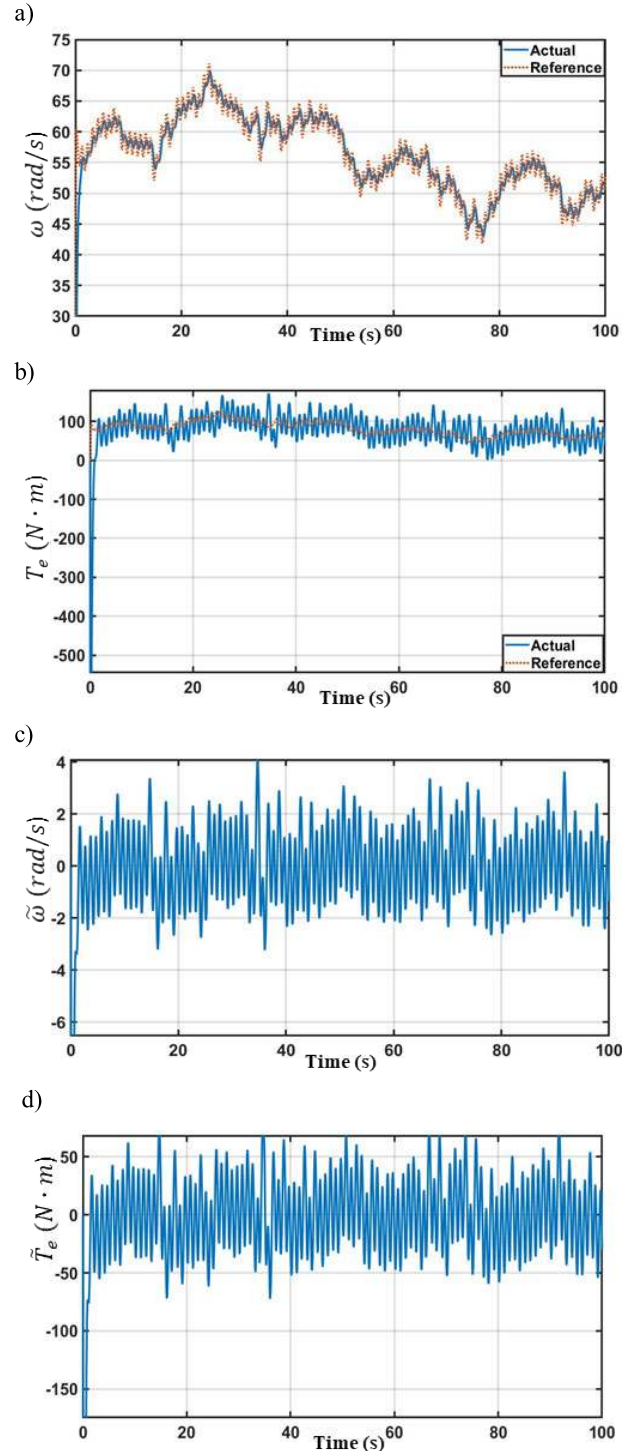
a)

b)

c)

d)

FIGURE 8. Scenario 2: (a) ω, angular shaft speed tracking (b) T_e, electromagnetic torque tracking (c) $\tilde{\omega}$ angular shaft speed tracking errors and (d) $\tilde{T}_e$, electromagnetic torque tracking with proposed control, N = 1.

In the Table 4, the proposed SDRE-based ISMC control system with $N = 1$ and $N = 2$ have been assessed and compared with other advanced control methods namely, LQR–based optimal control method published in [4], linear output feedback-based ISMC method [10], and switching output feedback control
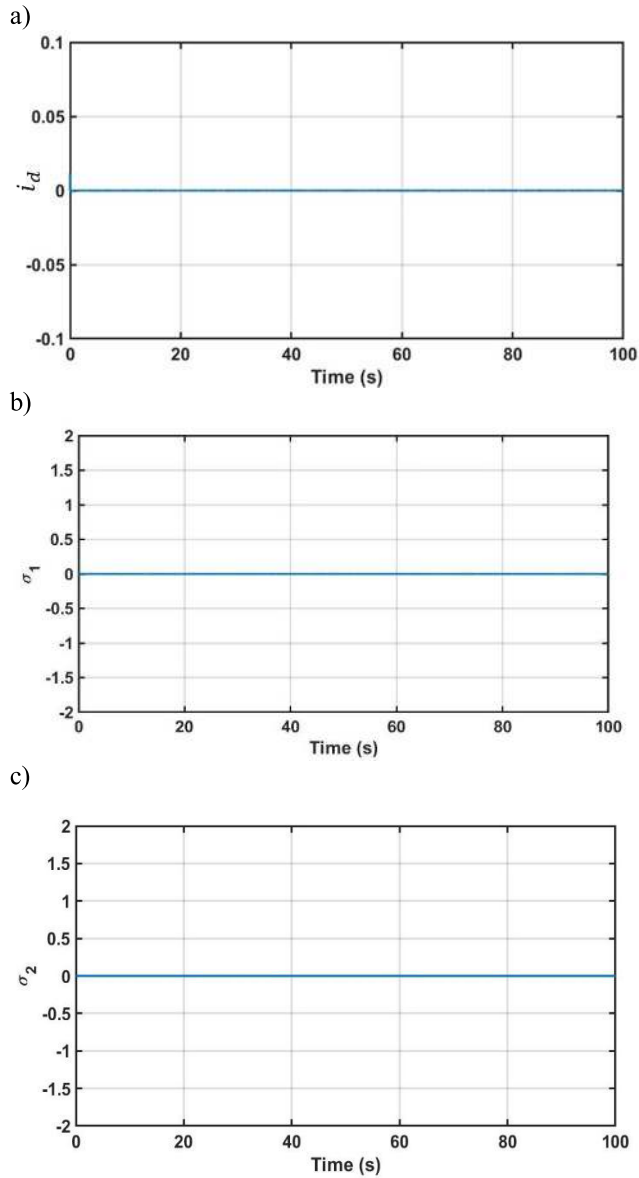
a)

b)

c)

FIGURE 9. Scenario 2: (a) i_d, d-axis current, (b) σ_1 sliding surface and (c) σ_2 sliding surface convergence to zero with proposed control, N = 1.

law based 1st order SMC method [29]. It should be noted that ISMC control method with $N = 0$ is same as linear output feedback–based ISMC proposed in [10].

Figs. 4-5 demonstrate the results of the proposed control method with $N = 1$, number of member of the Taylor's series. In fact, Fig. 4 shows reference angular shaft speed (ω_d), angular shaft speed response (ω), angular shaft speed tracking error ($\tilde{\omega}$), actual electromagnetic torque response (T_e), reference electromagnetic torque (T_{ed}), electromagnetic torque error ($\tilde{T}_e$), whereas in Fig. 5 d-axis current (i_d), q-axis sliding surface (σ_1), d-axis sliding surface (σ_2) are shown.

The same parameters (scenario 1) have been measured and shown for the proposed control method with $N = 2$ (Figs. 6-7). As it is difficult to observe the
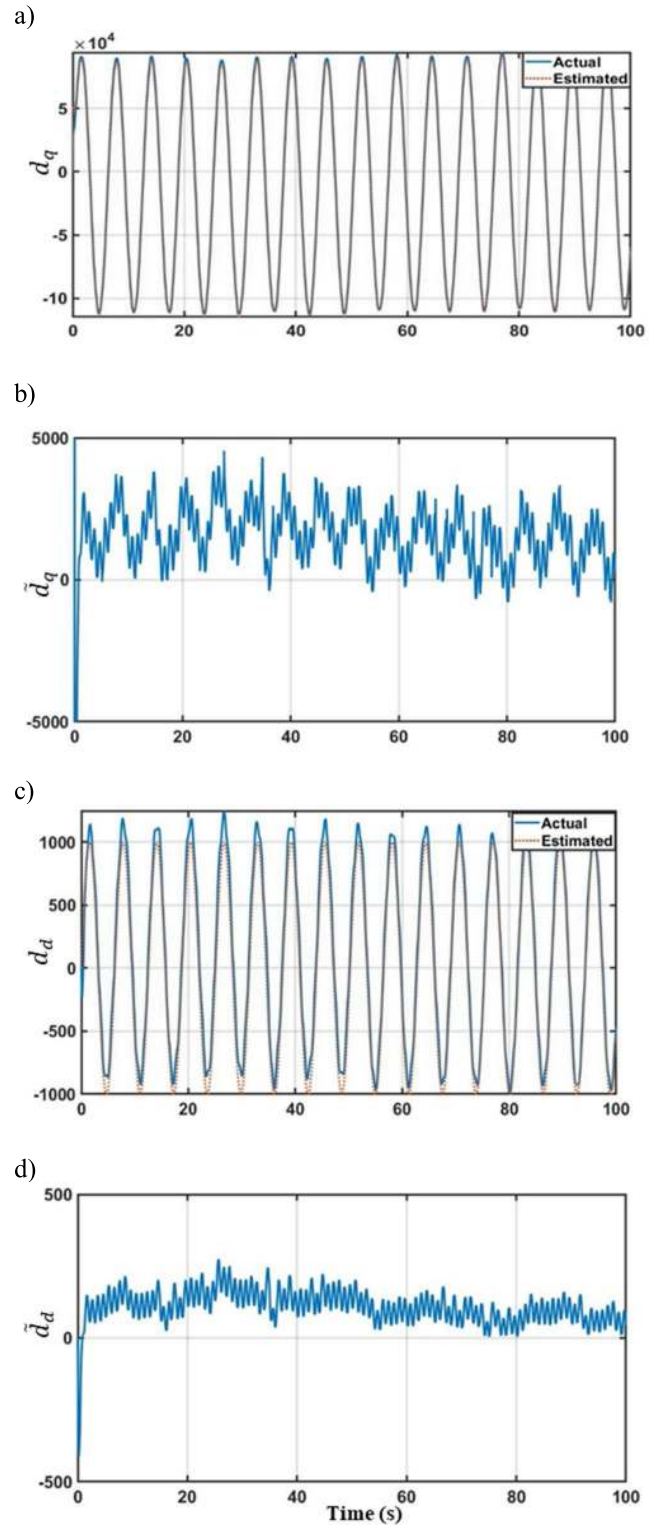
a)

b)

c)

d)

FIGURE 10. Scenario 2: (a) d_q and (c) d_d estimations and (b), (d) their errors with proposed control, N = 1.

difference visually, the proposed control performance has been compared by means of mean errors, where average angular shaft speed error is 0.0702% and average electromagnetic torque errors is 1.1709% for scenario 1 (Fig. 6). In fact, the average angular shaft speed tracking error is
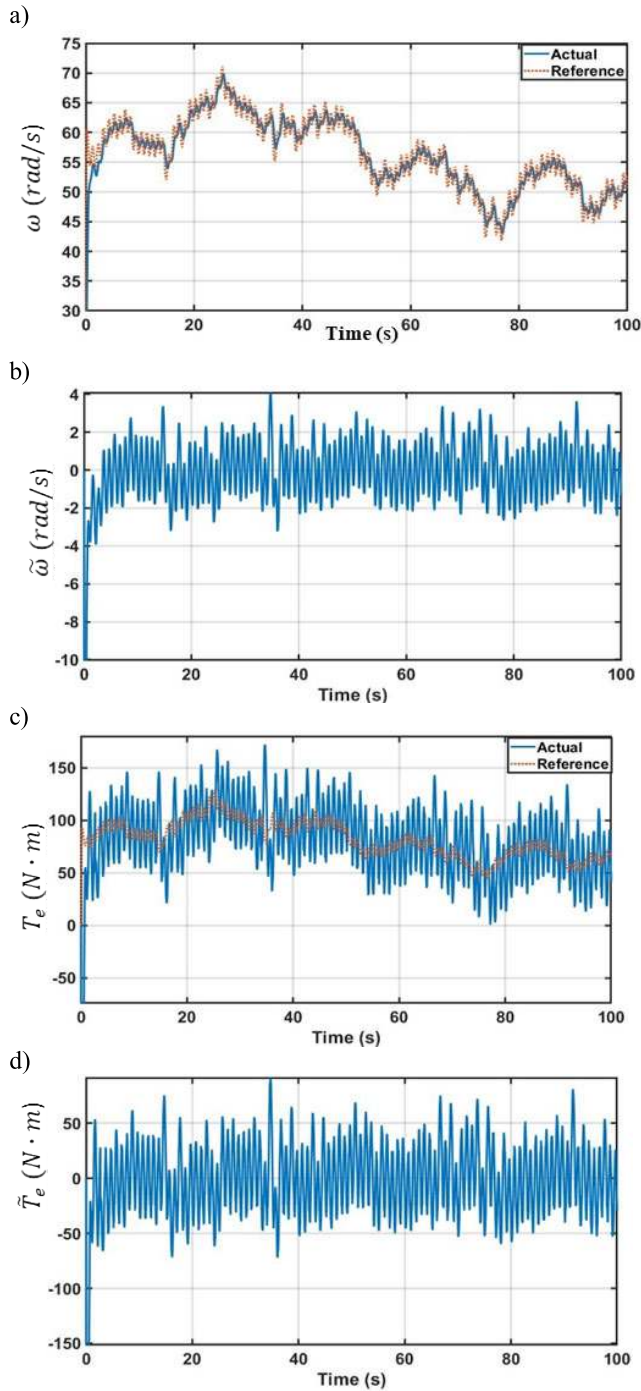
a)

b)

c)

d)

FIGURE 11. Scenario 2:(a) ω, angular shaft speed tracking, (b) $\tilde{\omega}$ angular shaft speed tracking errors (c) T_e, electromagnetic torque tracking and (d) $\tilde{T}_e$, electromagnetic torque tracking with proposed control, N = 2.

a)

b)

c)

FIGURE 12. Scenario 2: (a) i_d, d-axis current, (b) σ_1 sliding surface and (c) σ_2 sliding surface convergence to zero with proposed control, N = 2.

reduced for 0.16%/0.25%/0.25%/0.22% which better for 3.3/4.56/4.54/4.16 times than in the proposed control with N = 1 (Fig. 4), LQR, ISMC, SMC methods, respectively. The average electromagnetic torque error has been decreased for 2.4%/3.76%/3.74%3.66% which is better for 3.05/4.21/4.19/4.13 times than in the proposed control with N = 1 (Fig. 4), LQR, ISMC, SMC methods, respectively.

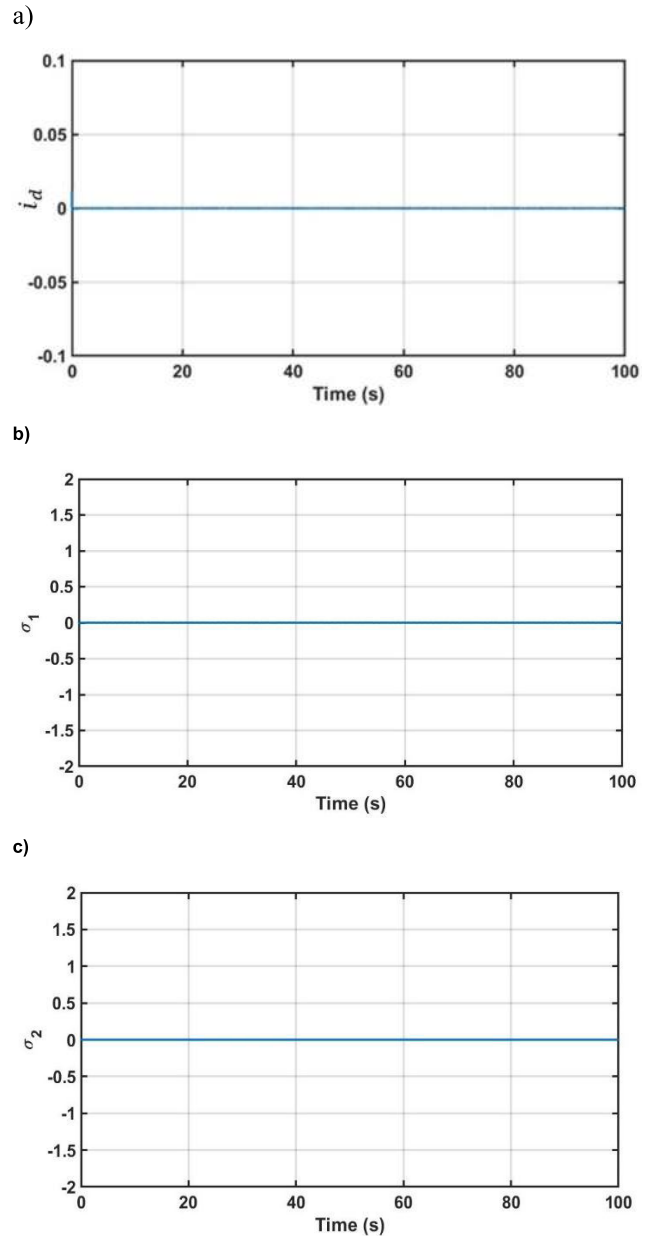The proposed method with $N = 2$ has been demonstrated robust performance under model uncertainty,

modelling errors and noise, which have been introduced in Scenario 2 (Figs. 8-13). The average angular shaft speed error composes 0.0621% and average electromagnetic torque error constitutes 1.0398% (Fig. 11). In fact, the average angular shaft speed error is reduced for 0.17%/0.26%/0.26%/0.23% which is better for 3.76/5.16/512/4.7 times. The average electromagnetic torque error is decreased for 2.55%/3.88%/3.85%/3.79% which is better for 3.46/4.74/4.71/4.65 times than in the proposed control with $N = 1$ (Fig. 8), LQR, ISMC, SMC methods, respectively.

In both scenarios, the proposed control method with $N = 1$ and $N = 2$ both sliding variables converge to zero (Fig. 5, Fig. 7, Fig. 9 and Fig. 12). As indicated in [41],
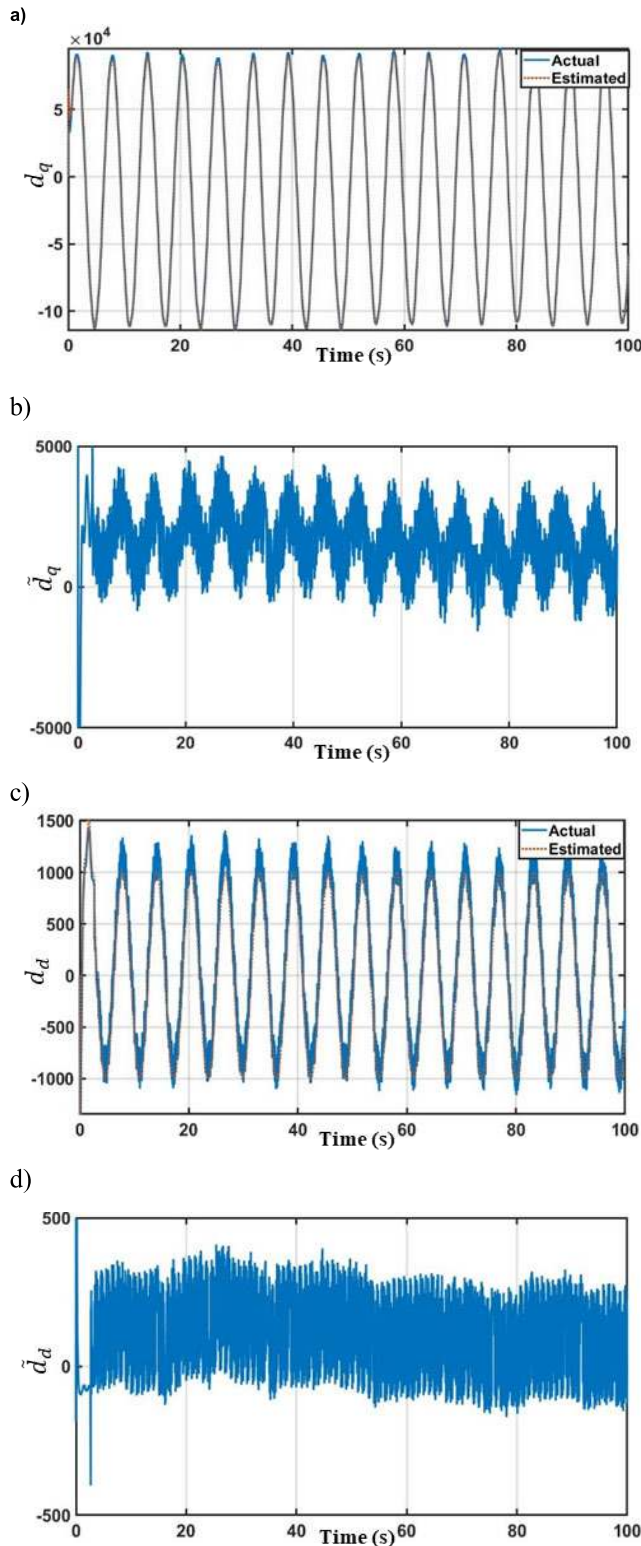
a)

b)

c)

d)

FIGURE 13. Scenario 2: (a) d_q and (c) d_d estimations and (b), (d) their errors with proposed control, N = 2.

the SDRE-based controller with N smaller than 2 is not complicated than cascade PI controller for permanent magnet synchronous machines. Further increasing Q and reducing R can improve the tracking performance, but according to

optimal control theories, more control effort is required. Moreover, further increasing terms in the series (N) can also help to improve control performance but at the same time put more burden on the computational complexity. Switching gains of sliding mode control, ρ_1 and ρ_2, also affect to the convergence rate of angular shaft speed of the PMSG, but over-tuning of these gains should be avoided.

In the scenario 2 actual q-axis disturbance (d_q), q-axis disturbance estimation ($\hat{d}_q$), actual d-axis disturbance (d_d), d-axis disturbance estimation ($\hat{d}_d$) have been measured to demonstrate robustness of the proposed control design under model uncertainty, modelling errors and noise (Figs. 10-13.).

From these results, it can be concluded that applying the proposed control method with GHODO observer can give more robust performance than with traditional anemometers–based control system.

VI. CONCLUSION

Efficient control of the variable-speed WECSs operation is highly important, since it allows to maximize the power outputs and provide safe operation of WECS.

The proposed SDRE-based ISMC for PMSG-based WECS application consists of SDRE–based nonlinear output feedback control technique as nominal part and continuously approximated integral-based switching function as discontinuous part. While the discontinuous part of ISMC eliminates reaching phase and reject matched disturbances, SDRE–based nonlinear output feedback facilitates closed-loop system stability with accurate approximation of nonlinear dynamics, which leads to better performance of the controller.

The proposed technique demonstrates better results than linear technique such as LQR, and nonlinear techniques as first order SMC, linear output feedback-based ISMC. The control method also has shown better response under fast changing external disturbance, model uncertainty, noise, and modelling errors.

According to our investigation, the limitations of this proposed control method are: 1) there is no detailed guidelines on how to select the approximated series number N. This value should be selected by trial-and-error technique through extensive simulation studies; 2) the control performance is affected by not only the weighting matrices *Q*, *R*, and series number *N*, but also their interaction. Thus this is still an open issue for this control method.

Applying the proposed SDRE-based ISMC technique to the grid–side converter's outputs with pitch control might be a following step of the research. Yet complex stability analysis is required to guarantee stability under different operation scenarios of the system.

REFERENCES

[1] V. Yaramasu, B. Wu, P. C. Sen, S. Kouro, and M. Narimani, "High-power wind energy conversion systems: State-of-the-art and emerging technologies," *Proc. IEEE*, vol. 103, no. 5, pp. 740–788, May 2015, doi: 10.1109/JPROC.2014.2378692.

[2] C.-H. Lin, "Novel modified Elman neural network control for PMSG system based on wind turbine emulator," *Math. Problems Eng.*, vol. 2013, May 2013, Art. no. 753756, doi: 10.1155/2013/753756.
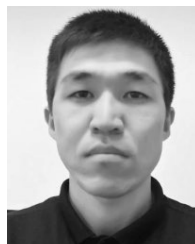
[3] R. Errouissi, A. Al-Durra, and M. Debouza, "A novel design of PI current controller for PMSG-based wind turbine considering transient performance specifications and control saturation," *IEEE Trans. Ind. Electron.*, vol. 65, no. 11, pp. 8624–8634, Nov. 2018, doi: 10.1109/TIE.2018.2814007.

[4] A. V. Le and T. D. Do, "High-order observers-based LQ control scheme for wind speed and uncertainties estimation in WECSs," *Optim. Control Appl. Methods*, vol. 39, no. 5, pp. 1818–1832, Sep. 2018, doi: 10.1002/oca.2444.

[5] V. P. Vu and T. D. Do, "A novel nonlinear observer-based LQ control system design for wind energy conversion systems with single measurement," *Wind Energy*, vol. 22, no. 8, pp. 1134–1147, Mar. 2019, doi: 10.1002/we.2345.

[6] V.-P. Vu and T. D. Do, "Observer-based LQR for wind energy conversion systems with single measurement," in *Proc. 4th Int. Conf. Green Technol. Sustain. Develop. (GTSD)*, Ho Chi Minh City, Vietnam, Nov. 2018, pp. 77–81.

[7] T. D. Do and H. T. Nguyen, "A generalized observer for estimating fast–varying disturbances," *IEEE Access*, vol. 6, pp. 28054–28063, 2018, doi: 10.1109/ACCESS.2018.2833430.

[8] T. D. Do, "Optimal control designfor chaos suppression of PM synchronous motors," in *Proc. 2nd Int. Conf. Control Sci. Syst. Eng. (ICCSSE)*, Singapore, Jul. 2016, pp. 88–92.

[9] A. Merabet, K. T. Ahmed, H. Ibrahim, and R. Beguenane, "Implementation of sliding mode control system for generator and grid sides control of wind energy conversion system," *IEEE Trans. Sustain. Energy*, vol. 7, no. 3, pp. 1327–1335, Jul. 2016, doi: 10.1109/TSTE.2016.2537646.

[10] K. Suleimenov, B. Sarsembayev, and T. Do, "Disturbance observer-based integral sliding mode control for wind energy conversion systems," *Wind Energy*, vol. 1, pp. 1–22, Jan. 2020, doi: 10.1002/we.2471.

[11] Y. Wang, W. Zhou, J. Luo, H. Yan, H. Pu, and Y. Peng, "Reliable intelligent path following control for a robotic airship against sensor faults," *IEEE/ASME Trans. Mechatronics*, vol. 24, no. 6, pp. 2572–2582, Dec. 2019, doi: 10.1109/tmech.2019.2929224.

[12] R. Errouissi and A. Al-Durra, "A novel PI-type sliding surface for PMSG-based wind turbine with improved transient performance," *IEEE Trans. Energy Convers.*, vol. 33, no. 2, pp. 834–844, Jun. 2018, doi: 10.1109/TEC.2017.2776752.

[13] H. H. H. Mousa, A.-R. Youssef, and E. E. M. Mohamed, "Optimal power extraction control schemes for five-phase PMSG based wind generation systems," *Eng. Sci. Technol., Int. J.*, vol. 23, no. 1, pp. 144–155, Feb. 2020, doi: 10.1016/j.jestch.2019.04.004.

[14] A. Shafiei, B. M. Dehkordi, A. Kiyoumarsi, and S. Farhangi, "A control approach for a small-scale PMSG-based WECS in the whole wind speed range," *IEEE Trans. Power Electron.*, vol. 32, no. 12, pp. 9117–9130, Dec. 2017, doi: 10.1109/TPEL.2017.2655940.

[15] Z. Ma, Z. Yan, M. L. Shaltout, and D. Chen, "Optimal real-time control of wind turbine during partial load operation," *IEEE Trans. Control Syst. Technol.*, vol. 23, no. 6, pp. 2216–2226, Nov. 2015, doi: 10.1109/TCST.2015.2410735.

[16] I. Jlassi, S. K. E. Khil, and N. M. Bellaaj, "Power switch and current sensor fault-tolerant control of PMSG drives for wind turbine systems," in *Proc. IEEE 10th Int. Symp. Diag. for Electr. Mach., Power Electron. Drives (SDEMPED)*, Guarda, Portugal, Sep. 2015, pp. 401–407.

[17] Z. Zhang, Z. Li, M. P. Kazmierkowski, J. Rodriguez, and R. Kennel, "Robust predictive control of three-level NPC Back-to-Back power converter PMSG wind turbine systems with revised predictions," *IEEE Trans. Power Electron.*, vol. 33, no. 11, pp. 9588–9598, Nov. 2018, doi: 10.1109/TPEL.2018.2796093.

[18] X.-X. Yin, Y.-G. Lin, W. Li, H.-W. Liu, and Y.-J. Gu, "Fuzzy-logic sliding-mode control strategy for extracting maximum wind power," *IEEE Trans. Energy Convers.*, vol. 30, no. 4, pp. 1267–1278, Dec. 2015, doi: 10.1109/TEC.2015.2422211.

[19] T. D. Do, "Disturbance observer-based fuzzy SMC of WECSs without wind speed measurement," *IEEE Access*, vol. 5, pp. 147–155, 2017, doi: 10.1109/ACCESS.2016.2633271.

[20] Y. Wang, H. Shen, H. R. Karimi, and D. Duan, "Dissipativity-based fuzzy integral sliding mode control of continuous-time T-S fuzzy systems," *IEEE Trans. Fuzzy Syst.*, vol. 26, no. 3, pp. 1164–1176, Jun. 2018, doi: 10.1109/TFUZZ.2017.2710952.

[21] Y. Wang, Y. Xia, H. Shen, and P. Zhou, "SMC design for robust stabilization of nonlinear Markovian jump singular systems," *IEEE Trans. Autom. Control*, vol. 63, no. 1, pp. 219–224, Jan. 2018, doi: 10.1109/TAC.2017.2720970.

[22] A. Kaibaldiyev, Y. Zhetpissov, B. Sarsembayev, and T. D. Do, "Combined H-∞ and integral sliding mode controllers for robust speed control of permanent magnet synchronous motor with load torque observer," in *Proc. Int. Conf. Syst. Sci. Eng. (ICSSE)*, Dong Hoi City, Vietnam, Jul. 2019, pp. 554–559.

[23] X.-H. Chang, R.-R. Liu, and J. H. Park, "A further study on output feedback H∞ control for discrete-time systems," *IEEE Trans. Circuits Syst. II, Exp. Briefs*, vol. 67, no. 2, pp. 305–309, Feb. 2020, doi: 10.1109/tcsii.2019.2904320.

[24] H. Wang, P. Xiaoping Liu, X. Xie, X. Liu, T. Hayat, and F. E. Alsaadi, "Adaptive fuzzy asymptotical tracking control of nonlinear systems with unmodeled dynamics and quantized actuator," *Inf. Sci.*, to be published, doi: 10.1016/j.ins.2018.04.011.

[25] L. Ma, X. Huo, X. Zhao, and G. D. Zong, "Observer-based adaptive neural tracking control for output-constrained switched MIMO nonstrict-feedback nonlinear systems with unknown dead zone," *Nonlinear Dyn.*, vol. 99, no. 2, pp. 1019–1036, Jan. 2020, doi: 10.1007/s11071-019-05322-w.

[26] H. Jafarnejadsani and J. Pieper, "Gain-scheduled ℓ₁-optimal control of Variable-Speed-Variable-Pitch wind turbines," *IEEE Trans. Control Syst. Technol.*, vol. 23, no. 1, pp. 372–379, Jan. 2015, doi: 10.1109/TCST.2014.2320675.

[27] K. D. Young, V. I. Utkin, and U. Ozguner, "A control engineer's guide to sliding mode control," *IEEE Trans. Control Syst. Technol.*, vol. 7, no. 3, pp. 328–342, May 1999.

[28] V. I. Utkin, "Sliding mode control design principles and applications to electric drives," *IEEE Trans. Ind. Electron.*, vol. 40, no. 1, pp. 23–36, Feb. 1993, doi: 10.1109/41.184818.

[29] B. Sarsembayev, T. Kalganova, A. Kaibaldiyev, T. Duc Do, and Y. Zhetpissov, "Sliding mode control with high-order disturbance observer design for disturbance estimation in SPMSM," in *Proc. Int. Conf. Syst. Sci. Eng. (ICSSE)*, Dong Hoi, Vietnam, Jul. 2019, pp. 542–547.

[30] C. A. Evangelista, A. Pisano, P. Puleston, and E. Usai, "Receding horizon adaptive second-order sliding mode control for doubly-fed induction generator based wind turbine," *IEEE Trans. Control Syst. Technol.*, vol. 25, no. 1, pp. 73–84, Jan. 2017, doi: 10.1109/TCST.2016.2540539.

[31] Y. Wang, Y. Xia, H. Li, and P. Zhou, "A new integral sliding mode design method for nonlinear stochastic systems," *Automatica*, vol. 90, pp. 304–309, Apr. 2018, doi: 10.1016/j.automatica.2017.11.029.

[32] Y. Shtessel, C. Edwards, L. Fridman, and A. Levant, "Introduction: Intuitive theory of sliding mode control," in *Sliding Mode Control and Observation*, 1st ed. New York, NY, USA: Springer, 2014, pp. 1–41.

[33] S. Kim and S. Kwon, "Nonlinear optimal control design for underactuated two-wheeled inverted pendulum mobile platform," *IEEE/ASME Trans. Mechatronics*, vol. 22, no. 6, pp. 2803–2808, Dec. 2017, doi: 10.1109/TMECH.2017.2767085.

[34] T. D. Do, H. H. Choi, and J.-W. Jung, "Nonlinear optimal DTC design and stability analysis for interior permanent magnet synchronous motor drives," *IEEE/ASME Trans. Mechatronics*, vol. 20, no. 6, pp. 2716–2725, Dec. 2015, doi: 10.1109/TMECH.2015.2426725.

[35] B. Stellato, T. Geyer, and P. J. Goulart, "High-speed finite control set model predictive control for power electronics," *IEEE Trans. Power Electron.*, vol. 32, no. 5, pp. 4007–4020, May 2017, doi: 10.1109/TPEL.2016.2584678.

[36] A. Mehta and B. Bandyopadhyay, "Preliminaries of Sliding Mode Control," in *Frequency-Shaped Observer-Based Discrete-time Sliding Mode Control*, vol. 2. New Delhi, India: Springer, 2015, pp. 9–25, doi: 10.1007/978-81-322-2238-5.

[37] Q. Gao, L. Liu, G. Feng, and Y. Wang, "Universal fuzzy integral sliding-mode controllers for stochastic nonlinear systems," *IEEE Trans. Cybern.*, vol. 44, no. 12, pp. 2658–2669, Dec. 2014, doi: 10.1109/TCYB.2014.2313028.

[38] C.-C. Chen, S. S.-D. Xu, and Y.-W. Liang, "Study of nonlinear integral sliding mode fault-tolerant control," *IEEE/ASME Trans. Mechatronics*, vol. 21, no. 2, pp. 1160–1168, Apr. 2016, doi: 10.1109/TMECH.2015.2474700.

[39] A. Ferrara and G. P. Incremona, "Design of an integral suboptimal second-order sliding mode controller for the robust motion control of robot manipulators," *IEEE Trans. Control Syst. Technol.*, vol. 23, no. 6, pp. 2316–2325, Nov. 2015, doi: 10.1109/TCST.2015.2420624.

[40] K. Suleimenov, M. Hazrat Ali, and T. Duc Do, "Integral sliding mode controller design for permanent magnet synchronous machines," in *Proc. Int. Conf. Syst. Sci. Eng. (ICSSE)*, Dong Hoi City, Vietnam, Jul. 2019, pp. 548–553.

[41] T. D. Do, H. H. Choi, and J.-W. Jung, "SDRE-based near optimal control system design for PM synchronous motor," *IEEE Trans. Ind. Electron.*, vol. 59, no. 11, pp. 4063–4074, Nov. 2012, doi: 10.1109/TIE.2011.2174540.

[42] T. D. Do, S. Kwak, H. H. Choi, and J.-W. Jung, "Suboptimal control scheme design for interior permanent-magnet synchronous motors: An SDRE-based approach," *IEEE Trans. Power Electron.*, vol. 29, no. 6, pp. 3020–3031, Jun. 2014, doi: 10.1109/TPEL.2013.2272582.

[43] B. Qin, H. Sun, J. Ma, W. Li, T. Ding, Z. Wang, and A. Y. Zomaya, "Robust H_∞ control of doubly fed wind generator via state-dependent Riccati equation technique," *IEEE Trans. Power Syst.*, vol. 34, no. 3, pp. 2390–2400, May 2019, doi: 10.1109/TPWRS.2018.2881687.

[44] S. R. Nekoo, "Model reference adaptive state-dependent Riccati equation control of nonlinear uncertain systems: Regulation and tracking of free-floating space manipulators," *Aerosp. Sci. Technol.*, vol. 84, pp. 348–360, Jan. 2019, doi: 10.1016/j.ast.2018.10.005.

[45] S. M. H. Rostami, A. K. Sangaiah, J. Wang, and H.-J. Kim, "Real-time obstacle avoidance of mobile robots using state-dependent Riccati equation approach," *EURASIP J. Image Video Process.*, vol. 2018, no. 1, pp. 1–13, Dec. 2018, doi: 10.1186/s13640-018-0319-1.

[46] Y. Batmani, "On the design of event-triggered suboptimal controllers for nonlinear systems," *Asian J. Control*, vol. 20, no. 3, pp. 1303–1311, May 2018.

[47] T. D. Do, Y. N. Do, and P. D. Dai, "A robust suboptimal control system design of chaotic PMSMs," *Electr. Eng.*, vol. 100, no. 3, pp. 1455–1466, Sep. 2018, doi: 10.1007/s00202-017-0603-6.

[48] V. Yaramasu and B. Wu, *Model Predictive Control of Wind Energy Conversion Systems*. Piscataway, NJ, USA: IEEE Press, 2016, pp. 3–58, doi: 10.1002/9781119082989.

[49] C. Edwards, H. Alwi, M. T. Hamayun, C. Edwards, H. Alwi, and M. T. Hamayun, *Fault Tolerant Control Schemes Using Integral Sliding Modes*, vol. 61. Cham, Switzerland: Springer, 2016, pp. 17–36, doi: 10.1007/978-3-319-32238-4.

KANAT SULEIMENOV received the B.S. degree in engineering and technology from Kazakh-British Technical University, Almaty, Kazakhstan, in 2014, and the M.S. degree in mechanical engineering from Nazarbayev University, Nur-Sultan, Kazakhstan, in 2019, where he is currently pursuing the Ph.D. degree with the Department of Robotics and Mechatronics. From November 2014 to August 2015, he was with Coca-Cola Almaty Bottlers Company, where he served as an Operator on the production line. From 2016 to 2017, he worked as a Laboratory Technician with the Department of Mechanical Engineering, School of Engineering, Nazarbayev University. From February 2018 to August 2019, he worked as a Research Assistant with the Power Conversion and Motion Control Laboratory, under the supervision of Dr. Ton Duc Do. His current research interests include control of electric machine drives used in electric cars and wind energy conversion systems.

BOTAGOZ MIRZAGALIKOVA, photograph and biography not available at the time of publication.

BAYANDY SARSEMBAYEV received specialist qualification in railway automation and control from the Kazakh Academy of Transport and Communications, Almaty, Kazakhstan, in 2000, and the M.Sc. degree in systems and control engineering from City University London, London, U.K., in 2015. He is currently pursuing the Ph.D. degree in electrical engineering and electronics research with Brunel University London, U.K.

From June 2000 to December 2000, he was with Kazakhstan National Railway Company, Karagandy, Kazakhstan, as a railway worker in Signals' systems. From 2001 to 2007, he was with the Kazakh Academy of Transport and Communications, Almaty, as a Teaching Staff in transport studies. From 2008 to 2012, he was with L.N. Gumilyov Eurasian National University, Astana, Kazakhstan, as a Teaching Staff in transport studies. Since July 2017, he has been a Research Assistant with the Department of Robotics and Mechatronics, Nazarbayev University, Astana. As RA in the Department of Robotics and Mechatronics, he investigates various control techniques and methods and applies them to Permanent Magnet Synchronous Motors and WECS applications. His research interests include, but not limited to, adaptive PID, vector control (field-oriented control), observer design for disturbance estimation, sliding mode control (SMC), and integral SMC.

TON DUC DO (Senior Member, IEEE) received the B.S. and M.S. degrees in electrical engineering from the Hanoi University of Science and Technology, Hanoi, Vietnam, in 2007 and 2009, respectively, and the Ph.D. degree in electrical engineering from Dongguk University, Seoul, South Korea, in 2014. From 2008 to 2009, he worked at the Division of Electrical Engineering, Thuy Loi University, Vietnam, as a Lecturer. He was at the Division of Electronics and Electrical Engineering, Dongguk University, as a Postdoctoral Researcher, in 2014. He was also a Senior Researcher at the Pioneer Research Center for Controlling Dementia by Converging Technology, Gyeongsang National University, South Korea, from May 2014 to August 2015. Since September 2015, he has been an Assistant Professor with the Department of Robotics and Mechatronics, Nazarbayev University, Kazakhstan. His research interests include the field of advanced control system theories, electric machine drives, renewable energy conversion systems, uninterruptible power supplies, electromagnetic actuator systems, targeted drug delivery systems, and nanorobots. He received the Best Research Award from Dongguk University, in 2014. He was also the Lead Guest Editor for special issue for the special issue of Mathematical Problems in Engineering on "Advanced Control Methods for Systems with Fast-Varying Disturbances and Applications." He is currently an Associate Editor of IEEE Access.

● ● ●